J Mater Sci: Mater Electron (2012) 23:1087–1093
DOI 10.1007/s10854-011-0553-0

Deposition and optoelectronic properties of ITO (In_2O_3:Sn) thin films by Jet nebulizer spray (JNS) pyrolysis technique

N. Sethupathi · P. Thirunavukkarasu · V. S. Vidhya · R. Thangamuthu · G. V. M. Kiruthika · K. Perumal · Hari C. Bajaj · M. Jayachandran

Received: 26 August 2011 / Accepted: 14 October 2011 / Published online: 30 October 2011

Abstract Nanocrystalline ITO thin films were deposited on glass substrates by a new spray pyrolysis route, Jet nebulizer spray (JNS) pyrolysis technique, for the first time at different substrate temperatures varying from 350 to 450 °C using a precursor containing indium and tin solution with 90:10 at% concentration. The structural, optical and electrical properties have been investigated as a function of temperature. X-ray diffraction analysis showed that the deposited films were well crystallized and polycrystalline with cubic structure having (222) preferred orientation. The optical band gap values calculated from the transmittance spectra of all the ITO films showed a blue shift of the absorbance edge from 3.60 to 3.76 eV revealing the presence of nanocrystalline particles. AFM analysis showed uniform surface morphology with very low surface roughness values. XPS results showed the formation of ITO films with In^{3+} and Sn^{4+} states. TEM results showed the nanocrystalline nature with grain size about 12-15 nm and SAED pattern confirmed cubic structure of the ITO films. The electrical parameters like the resistivity, mobility and carrier concentration are found as 1.82×10^{-3} Ω cm, 8.94 cm^2/Vs and 4.72×10^{20} cm^{-3}, respectively for ITO film deposited at 400 °C. These results show that the ITO films, prepared using the new JNS pyrolysis technique, have the device quality optoelectronic properties when deposited under the proposed conditions at 400 °C.

N. Sethupathi
Department of Physics, Arignar Anna Government Arts College, Namakkal 637 002, India

P. Thirunavukkarasu
Department of Electronics, SRMV College of Arts and Science, Coimbatore 641 020, India

V. S. Vidhya
Department of Chemistry, Chendhuran College of Engineering and Technology, Pudukkottai 622 507, India

R. Thangamuthu · G. V. M. Kiruthika · M. Jayachandran (✉)
Electrochemical Materials Science Division, CSIR-Central Electrochemical Research Institute, Karaikudi 630006, India
e-mail: mjayam54@yahoo.com

K. Perumal
Department of Physics, SRMV College of Arts and Science, Coimbatore 641 020, India

H. C. Bajaj
Discipline of Inorganic Materials and Catalysis, CSIR-Central Salt and Marine Chemicals Research Institute, Bhavnagar 364021, India

1 Introduction

Thin film semiconductors that are exhibiting simultaneously high optical transmittance and low electrical resistivity have seminal importance in technologically important devices, for instance in solar cells and in various optoelectronic devices, light emitting diodes etc. [1–3]. It is known that Indium tin oxide (ITO) material is a degenerate n-type semiconductor and is the most suitable oxide thin film for the above mentioned as well as many other applications. The ITO has proven to be an advanced semiconducting material opening a new window in many electronic and optical industries due to its large optical bandgap and the plasma frequency lying in the near IR spectral region [4]. Due to such special characters and salient features, ITO shows excellent transparency in the visible region but is fairly reflective in the infrared spectral regions. In_2O_3 is an insulator in its stoichiometric form and a conductor in its non-stoichiometric form with a wide direct bandgap of about 3.60 eV [5]. This high electrical

conductivity arises from the formation of a conducting carrier-oxygen vacancy with the addition of a dopant, tetravalent cation Sn^{4+}, to the In_2O_3 matrix. The oxygen vacancies act as doubly-ionized donors and contribute a maximum of two electrons to the electrical conductivity. Over the past decades, many researchers have investigated the preparation of ITO thin films using various techniques, because of their wide utilization in fabricating solar cells [6].

The preparation techniques of ITO thin films have come to play an important role to decide their characteristics and in obtaining highly crystalline, stress free and morphologically uniform films on flexible or suitable substrates for many applications [7]. In this regard, deposition of metal oxide films with nanoparticles at relatively lower temperatures is a prerequisite for developing transparent conducting oxide based optoelectronic devices.

Techniques employing liquid-phase aqueous/alcoholic solutions have the advantages of simple operation, low-cost instrumentation, easy doping, and controllable particle size, which can produce atomic level mixing. Such techniques include spray pyrolysis, dip-coating, sol–gel, wet-chemical, and liquid-phase [8–13]. The spray pyrolysis technique is widely adopted owing to its cost effectiveness and large area applicability. The critical and efficient operation of the spray pyrolysis technique depends on the preparation of uniform sized fine droplets followed by the controlled thermal decomposition of these droplets in terms of environment, location and time. Generally, commercialized nozzle spray guns are used to spray and such nozzle atomizers are neither sufficient to generate submicron or nano size droplets reproducibly nor to control their size distribution. Consequently, some new and modified spray atomization techniques have been developed recently and used effectively for thin film preparation [14].

In this context, the Jet nebulizer, a new type of atomizer, is found to be very promising for the fabrication of ITO films with low resistivity and high transmittance possessing nano crystalline particles. In this paper, we present and discuss the first preliminary results on the investigation of the structural, electrical, optical and morphological properties of ITO films deposited by the new Jet nebulizer spray (JNS) pyrolysis technique.

2 Experimental

The Indium tin oxide (ITO) thin films were prepared by taking Indium(III) acetate (0.1 M) and Tin (II) acetate (0.1 M) in the atomic composition ratio of 90%/10% for indium/tin and keeping the substrate temperature range of 350–450 °C in steps of 25 °C. The first chemical indium acetate and an appropriate % of tin acetate were dissolved in 50 mL of deionised water with a rapid stirring and a few drops of concentrated HCl was added for getting a clear solution, which was heated to about 60 °C for complete dissolution.

Figure 1 shows the experimental set-up of Jet nebulizer spray (JNS) pyrolysis technique, which comprises an air compressor with control valve, the main technical unit of Jet Nebulizer assembly, a mist carrier tube with a conical spray nozzle and an electrical heater attached with temperature controller. The Jet nebulizer is a small atomizing machine, which acquires the ability to convert the precursor solution into very tiny droplets by double collision process, when powered by an air compressor. In the atomizer unit the compressed air is released through the Jet nozzle of 0.5 mm diameter and it produces consisting of sub micron size droplets and aerosol mist formed and delivered through the carrier tube nozzle. When the aerosol

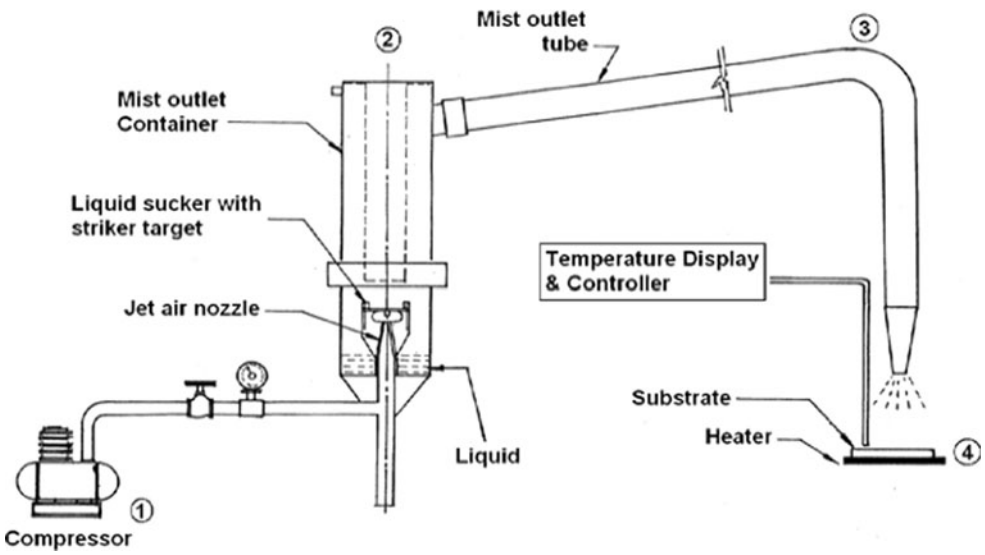

Fig. 1 Schematic diagram of the Jet Nebulizer spray (JNS) pyrolysis setup: (*1*) air compressor, (*2*) Jet nebulizer assembly, (*3*) mist outlet tube and (*4*) heater with temperature controller

mist touches the heated glass substrate, evaporation of solvent takes place followed by a heterogeneous reaction, which leads to the formation of oxide thin film on the substrate.

The deposition parameters, optimized by many trials [15] are: air pressure = 3.5 kg/cm^2, nozzle to substrate distance = 5 cm, rate of spray = 0.75 mL/min. The solution was sprayed for 10 min by the Jet nebulizer air flow through a specially designed carrier tube on to heated glass substrates held at constant temperature between 350 and 450 °C. The glass substrates of 2.5 × 2.5 cm^2 area were first cleaned by a liquid detergent, washed with distilled water, kept in freshly prepared hot chromic acid for 30 min, again thoroughly cleaned with distilled water and finally subjected to ultrasonic cleaning for 30 min just before the deposition of ITO films. Thickness of the ITO films was measured by the Stylus Profilometer (Mitutoyo), which were found in the range of 360–380 nm.

The structural properties of the ITO thin films were studied by X-ray diffractometer (X'pert Pro PANalytical-3040 using CuK_α radiation) with the wave length of = 1.5406 Å. The optical transitions of deposited films were determined using a UV–Vis-NIR double beam spectrometer (Hitatchi-330). The electrical properties of the ITO films were measured by the four probe setup (Scientific model DEP-02). The surface morphology and roughness of the films were analyzed using a Nanoscope E-3138j AFM/STM atomic force microscope (AFM). Analysis of chemical state of elements was determined using a Multilab 2000 X-ray photoelectron spectroscope (XPS) with MgK_α (1,253.6 eV) X-ray source. TEM image and selected area electron diffraction (SAED) pattern were recorded using a 200 kV Tecnai-20 G2 TEM Instrument.

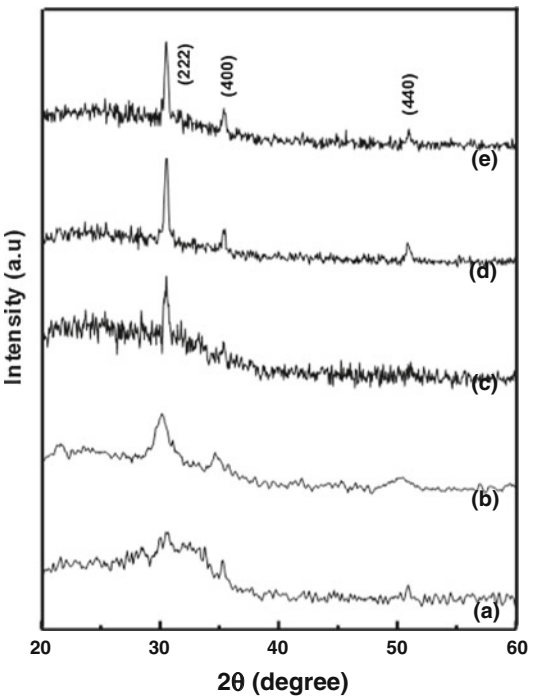

Fig. 2 XRD patterns of ITO films deposited at (*a*) 350, (*b*) 375, (*c*) 400, (*d*) 425 and (*e*) 450 °C

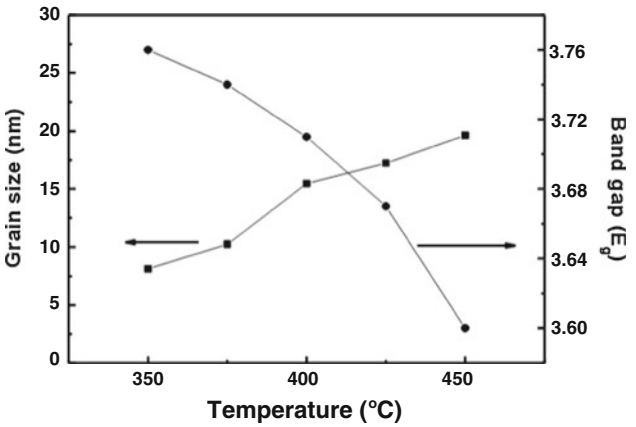

Fig. 3 Variation of grain size and bandgap (E_g) of ITO films deposited at different substrate temperatures

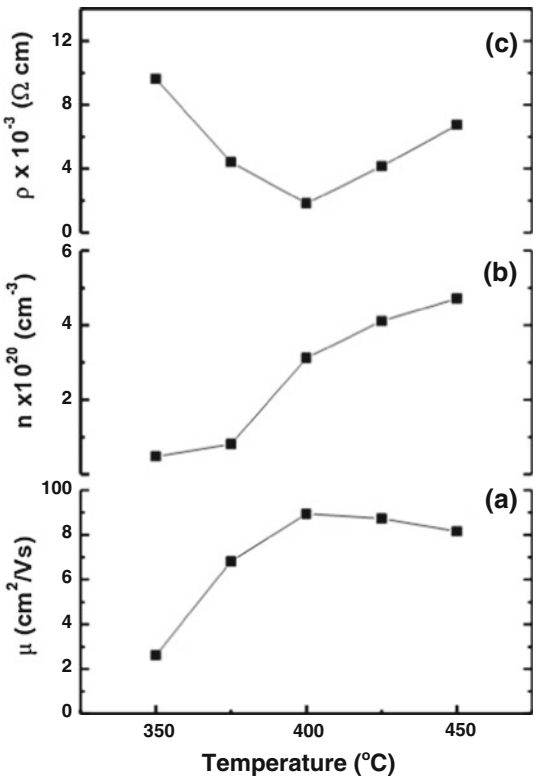

Fig. 4 Variation of (*a*) mobility, μ (*b*) carrier concentration, n and (*c*) resistivity, ρ for the ITO films prepared at various substrate temperatures

3 Results and discussions

Figure 2 shows the X-ray diffraction spectra of Jet nebulizer sprayed ITO films deposited at different substrate temperatures of 350–450 °C. The analysis of crystal structure revealed that the films were identified as crystallized cubic ITO. In the XRD patterns, peaks appearing at 2θ values 30.52°, 35.36° and 50.75° are due to reflections from (222), (400) and (440) planes of ITO respectively. The peak intensity of (222) plane was predominant among the other reflection planes indicating the preferential orientation of the ITO films. There are no peaks pertaining to SnO_2 or SnO at 26.5° or 33.2°, indicating the complete miscibility of In and Sn in the ITO films prepared here [16]. The grain size of the ITO thin films was calculated from the line broadening of the (222) diffraction line according to the Scherrer equation

$$D = 0.94\lambda / \beta \operatorname{Cos} \theta \quad (1)$$

where λ is the wavelength of the X-ray radiation and β is the diffraction broadening of the peak at the full width at half maximum (FWHM) and θ is the Bragg's angle. Variation of grain size and band gap (E_g) with substrate temperatures is shown in Fig. 3.

The lattice constant values were calculated and the values are found decreasing from 1.026 nm to 1.014 nm for the ITO films deposited at 350–450 °C, respectively.

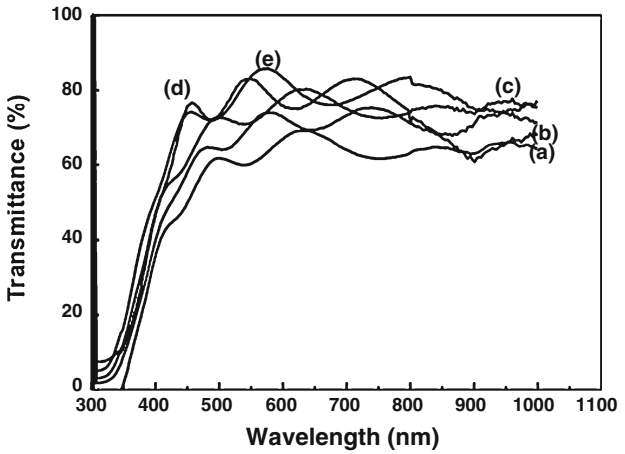

Fig. 5 Optical transmittance spectra of ITO films deposited at (*a*) 350, (*b*) 375, (*c*) 400, (*d*) 425 and (*e*) 450 °C

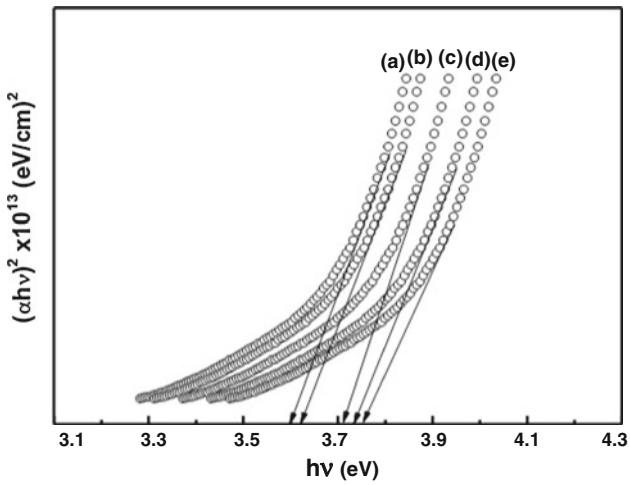

Fig. 6 Tauc plot of $(\alpha h\nu)^2$ versus hν for the ITO films deposited at different temperatures: (*a*) 350, (*b*) 375, (*c*) 400, (*d*) 425 and (*e*) 450 °C

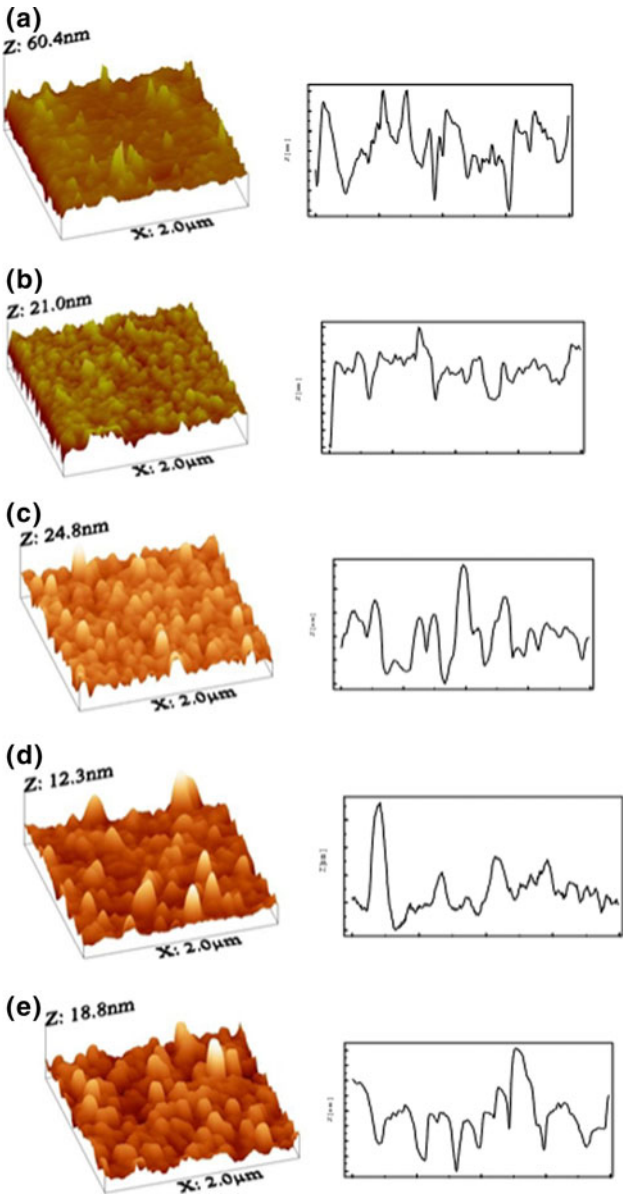

Fig. 7 AFM (3D images and surface line profiles) of ITO films deposited **a** 350, **b** 375, **c** 400, **d** 425 and **e** 450 °C

This decreasing trend shows an increased oxygen concentration in the ITO films, which reveals a relatively moderate resistivity (about 10^{-3} Ω cm) in the present case. This is also supported by the (222) preferential orientation in these films as observed from the XRD spectra. High oxygen incorporation and content (nearly stoichiometric) always leads to ITO films oriented in the (111) direction. But, in the present case, the carrier concentration is increasing with temperatures which may be due to the increased crystallinity, to the grain size increase with less grain boundary defects and also to the one-to-one substitution of In^{3+} ions with Sn^{4+} ions in the In_2O_3 lattice. Further, such a substitution led to an overall increase in the lattice parameter values of the ITO films compared to the standard value of a = 1.012 nm. This is attributed to an increase in repulsive forces arising from the extra positive charge of the Sn^{4+} cations and also to the interstitial oxygen anion charge compensation [17]. The grain size varies nominally from about 8.13 to 19.64 nm when the temperature was varied from 350 to 450 °C, respectively.

The electrical properties, resistivity (ρ), carrier concentration (N) and mobility (μ) of ITO films prepared by various substrate temperatures are presented in Fig. 4. The lowest resistivity is obtained at 400 °C and the corresponding value is 1.82×10^{-3} Ω cm. The value of carrier concentration reaches a maximum of 4.72×10^{20} cm^{-3} showing a continuous variation from 350 to 450 °C. The carrier mobility value reaches a maximum of 8.94 cm^2/Vs at 400 °C and then shows a decreasing trend.

The optical transmission spectra of ITO films deposited at different temperatures from 350 to 450 °C are shown in Fig. 5. All the ITO films show interference patterns showing that they are uniform and specular to a greater extent. The increase in the average transmittance value in the visible region from about 60 to 85% with temperature can be due to the well-crystallized lattice and the pinhole free surface of the ITO films. It is observed that transmission slope is shifted towards the short wavelength direction with (blue shift) the increase in deposition temperature, which is attributed to the increase of the carrier concentration with temperature [1].

The optical bandgap (E_g) values of these films were calculated using the Tauc plot [18] drawn using the equation:

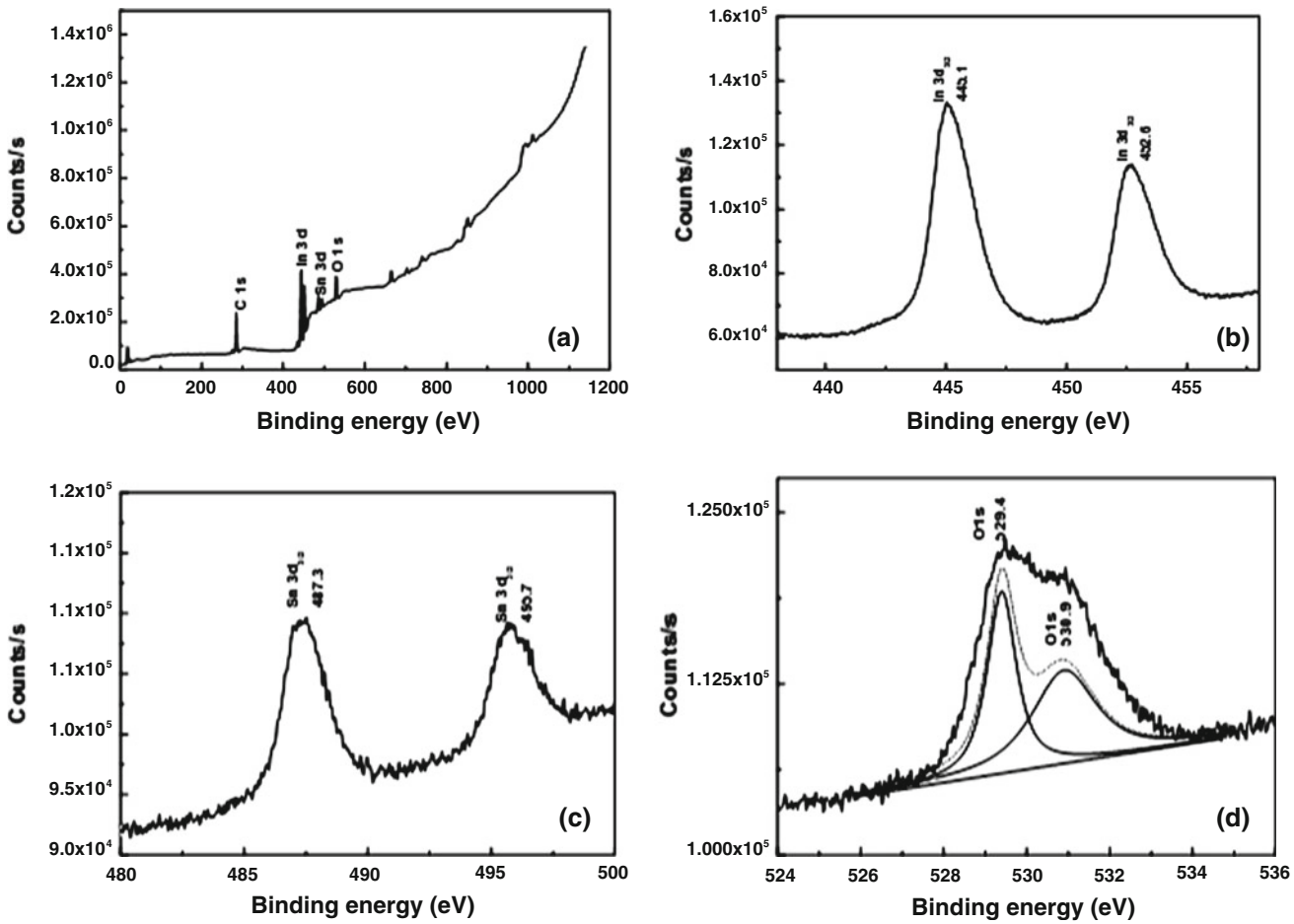

Fig. 8 XPS wide scan (**a**) and narrow scan spectra of In 3d (**b**), Sn 3d (**c**), O 1 s (**d**) peaks of ITO film deposited at 400 °C

$$\alpha h\nu = A\left(h\nu - E_g\right)^n \quad (2)$$

where α is the absorption coefficient, h is Planck's constant, ν is the frequency of the incident photon and n depends on the type of electron transition in the semiconductor film with 1/2 revealing the direct transition nature in the ITO films studied here. The absorption coefficient (α) was computed from the transmittance spectra using the relation, $I = I_o \exp(-\alpha t)$ from which α is obtained as = 1/t*ln(1/T), where t is the thickness of the film, I is the transmitted intensity of a particular wavelength through the film and I_o is the maximum transmitted intensity (100%).

The E_g values were estimated by extrapolating the straight line portion of the $(\alpha h\nu)^2$ versus $h\nu$ plots to $h\nu$ axis as shown in Fig. 6. The direct transition band gap values are found to be as 3.60, 3.64, 3.72, 3.74 and 3.76 eV for the ITO films deposited at 350, 375, 400, 425 and 450 °C, respectively. The bandgap value is 3.53 eV [19] for the bulk ITO material. The higher E_g values 3.60–3.76 eV observed here may be associated with the nanocrystalline nature of the ITO films deposited by the JNS pyrolysis route engaged in the present study.

Further, these enhanced band gap values come from the Burstein-Moss shift [20] represented as

$$E_g = E_{go} + \Delta E_{BM} = E_{go} + \hbar\left(3\pi^2 n\right)^{2/3}/2m^*_{vc} \quad (3)$$

where m^*_{vc} is the reduced effective mass, E_{go} is the band gap of the bulk material, n is the carrier concentration and E_g is the measured direct band gap value at different deposition temperature. From this expression it is clear that the blue shift depends on the increasing concentration values in the ITO films deposited here.

Figure 7 presents 3D AFM images, and the surface profiles of ITO films over a scanned area of 2 μm × 2 μm deposited at different temperatures of 350, 375, 400, 425 and 450 °C. The AFM images show that the ITO films are composed of densely packed columns perpendicular to the substrate. The grain size is found increasing with temperature and the ITO film deposited at 400 °C shows uniform surface morphology and grain size, while other surfaces show nonuniform grain size distribution and grains with varying heights. The AFM surface profile measurements yield increasing root mean square (rms) surface roughness values for the ITO films as 8.5, 10.2, 3.5, 6.8 and 5.4 nm with increasing temperature. It shows that the ITO films deposited at 400 °C have smoother surface and possess near-spherical nano particles that are uniformly distributed throughout the surface along with few columnar or elliptical shaped particles.

Figure 8 shows the XPS results of the ITO film deposited at 400 °C. Figure 8a shows the XPS survey scan showing the presence of peaks pertaining to In, Sn and O, which confirm the formation of ITO film. The narrow scan XPS spectra for the In 3d and Sn 3d doublet are shown in Fig. 8b and c, respectively. The binding energy of In $3d_{5/2}$ at 445.1 eV is attributed to the bonding between In^{3+}–O^{2-} from In_2O_3 lattice. The binding energy of Sn $3d_{5/2}$ is observed at 487.3 eV corresponding to the Sn^{4+}–O^{2-} bonding from the SnO_2 lattice. The O 1s spectrum has two peaks shown in Fig. 8d. The binding energy observed at 529.4 eV is assigned to lattice oxygen in the crystalline indium tin oxide and the peak at 531.6 eV corresponds to oxygen atoms in the amorphous ITO phase [21].

Figure 9a and b shows the TEM image and the selected area electron diffraction (SAED) pattern of the ITO film deposited at 400 °C. The TEM image (Fig. 9a) shows a homogenous distribution of ITO nanoparticles with diameter of about 12–15 nm. Individual as well as stacked particles are observed. This is in good agreement with the

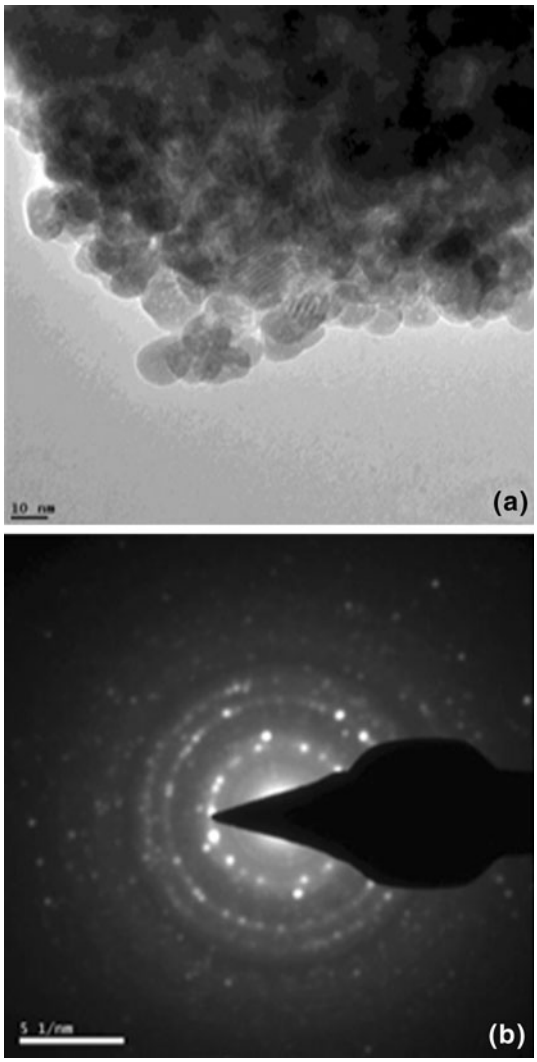

Fig. 9 TEM image (**a**) and SAED pattern (**b**) of ITO film deposited at 400 °C

particle size calculated from the XRD results. Figure 9b shows the SAED pattern exhibiting diffraction spots arranged on rings. This corresponds well to the granular grains observed in the AFM pictures and shows that the ITO film is well crystallized and polycrystalline in nature. The d-values obtained from this SAED pattern are in consistent with the XRD results and confirm the cubic structure.

4 Conclusions

Nanocrystalline ITO films have been deposited by simple and low cost Jet nebulizer spray pyrolysis technique for the first time. The influence of deposition temperature on the structural, optical and electrical properties was studied. The films are preferentially oriented along (222) plane with cubic structure. Highly transparent and low resistivity ITO films are obtained at 400 °C. For these films, both the band gap value and the carrier concentration are maximum revealing their nanocrystalline and well oriented nature. AFM and TEM results also confirm the nano grain morphology with uniform size distribution. These results show that the JNS pyrolysis technique can be used to prepared device quality ITO films with low resistivity, high transmittance in the visible region and wide band gap at relatively lower deposition temperature. Further work is in progress to optimize other deposition parameters, which will be presented in future publications.

References

1. C.G. Giranqurist, A. Hultaker, Thin Solid Films **411**, 1 (2002)
2. H.C. Lee, O. Ok Park, Vaccum **80**, 880 (2006)
3. A. Antony, M. Nisha, R. Manoj, M.K. Jayaraj, Appl. Surf. Sci. **225**, 294 (2004)
4. A. Ambrosini, A. Duarte, K.R. Poeppelemelier, M. Lank, C.R. Kannewurf, T.O. Mason, Solid State Chem. **153**, 41 (2000)
5. A. Antony, M. Nisha, R. Manoj, M.K. Jayaraj, Appl. Surf. Sci. **225**, 294 (2004)
6. S.J. Limmer, K. Takahashi, G. Cao, In: Proc SPIE **5224**, 25 (2003)
7. S. Takayama, A. Tanaka, T. Sugawara, T. Himuro, Jpn. J. Appl. Phys. **41**, L619 (2002)
8. P.S. Patti, Mater. Chem. Phys. **59**, 185 (1999)
9. P.K. Manoj, K.G. Gopchandran, B. Joseph, P. Kushy, V.K. Vaidyan, Indian J. Phys. **75A**, 507 (2001)
10. K. Soulantica, L. Erades, M. Souvan, F. Senocq, A. maisonnat, B. Chaudret, Adv. Funct. Mater. **13**, 553 (2003)
11. T. Ogi, F. Iskandar, Y. Itoh, K. Okuyama, J. Nanopart. Res. **8**, 343 (2006)
12. A. Nakata, M. Mizuhata, S. Deki, Electrochim. Acta **53**, 179 (2007)
13. J. Yang, C. Zhao, X. Liu, J. Yu, D. Sun, W. Tang, Chin. J. Chem. Eng. **19**, 179 (2011)
14. P.S. Patil, Mater. Chem. Phys **59**, 187 (1999)
15. P.K. Manoj, K.G. Gopchandran, Peter. koshy, V.K. Vaidyan, B. Joseph, Opt. Mater. **28**, 1405 (2006)
16. P. Sujatha Devi, M. Chatterjee, O. Ganguli, Mater. Lett **55**, 205 (2002)
17. G.G. Gonzalez, J.B. Cohen, J.H. Hwang, T.O. Mason, J. Appl. Phys. **87**, 2550 (2001)
18. R.W. Smith, J. Appl. Phys. **81**, 1196 (1997)
19. C.H.L. Weisitens, P.A.C. VanLoon, Thin Solid Films **196**, 1 (1991)
20. E. Burstein, Phys.Rev **93**, 632 (1954)
21. Y.-S. Kim, Y.-C. Park, S.G. Ansari, B.-S. Lee, H.-S. Shin, Thin Solid Films **426**, 124 (2003)